

Attosecond dynamics of electron scattering by an absorbing layer

R.O. Kuzian^{1,2} and E. E. Krasovskii^{1,3,4}

¹*Donostia International Physics Center (DIPC),*

20018 Donostia/San Sebastián, Basque Country, Spain

²*Institute for Problems of Materials Science NASU, Krzhizhanovskogo 3, 03180 Kiev, Ukraine*

³*Universidad del Pais Vasco/Euskal Herriko Unibertsitatea,*

20080 Donostia/San Sebastián, Basque Country, Spain

⁴*IKERBASQUE, Basque Foundation for Science, 48013 Bilbao, Basque Country, Spain*

Attosecond dynamics of electron reflection from a thin film is studied based on a one-dimensional jellium model. Following the Eisenbud-Wigner-Smith concept, the reflection time delay $\Delta\tau_r$ is calculated as the energy derivative of the phase of the complex reflection amplitude r . For a purely elastic scattering by a jellium slab of a finite thickness d the transmission probability T oscillates with the momentum K in the solid with a period π/d , and $\Delta\tau_r$ closely follows these oscillations. The reflection delay averaged over an energy interval grows with d , but in the limit of $d \rightarrow \infty$ the amplitude r becomes real, so $\Delta\tau_r$ vanishes. This picture changes substantially with the inclusion of an absorbing potential $-iV_i$: As expected, for a sufficiently thick slab the reflection amplitude now tends to its asymptotic value for a semi-infinite crystal. Interestingly, for $V_i \neq 0$, around the $T(E)$ maxima, the $\Delta\tau_r(E)$ curve strongly deviates from $T(E)$, showing a narrow dip just at the $\Delta\tau_r(E)$ maximum for $V_i = 0$. An analytical theory of this counterintuitive behavior is developed.

I. INTRODUCTION

Rapid progress in time-resolved electron spectroscopy, in particular in the experiments on attosecond streaking [1–8] and RABBITT interferometry [9, 10], has drawn the attention to microscopic theoretical approaches capable of underlying *ab initio* methods applicable to realistic solids. In contrast to stationary photoemission, where a steady flux of light causes steady photocurrent, the photoelectron excited by a short light pulse is naturally viewed as a wave packet that propagates through the medium toward the detector. One fruitful approach to the propagation timing stems from the concept of Eisenbud-Wigner-Smith time delay [11–13], which allows to express the asymptotic equation of motion in terms of stationary states, namely as the energy derivative of the scattering phase.

Consider a wave packet composed of plane waves with the wave vectors along \mathbf{z} : For a finite scatterer, the maximum of the incident wave packet asymptotically far from the scatterer has the equation of motion $z_i(t) = vt$, where $v = \hbar k/m$ is the group velocity of the free motion. Behind the scatterer, the transmitted wave packet obeys the asymptotic equation of motion

$$z_T(t) = v(t - \Delta\tau_{\text{EWS}}), \quad (1)$$

where $\Delta\tau_{\text{EWS}}$ is known as the phase time or Eisenbud-Wigner-Smith (EWS) time delay, and for a spectrally narrow wave packet it equals the energy derivative of the scattering phase η_T [11–13]:

$$\Delta\tau_{\text{EWS}} = \hbar d\eta_T/dE \equiv \dot{\eta}. \quad (2)$$

If the starting and the ending points are sufficiently far away from the scattering region then $\Delta\tau_{\text{EWS}}$ can be interpreted as the difference between the time needed by a free electron to transit the distance between the two

points and the actual time needed by the scattered electron. The problem of transit time has been addressed in numerous studies, with main attention paid to paradoxes related to elastic scattering, see review articles [14–17].

The implications of the inelastic scattering remain less studied despite its importance in electron spectroscopies: Electron damping leads to a finite electron escape depth in photoemission [18] and decreases reflectivity in the low energy electron diffraction (LEED) experiment [19]. The standard method to take into account electron damping used since it was suggested by Slater in 1937 [19] consists in adding an imaginary potential $-iV_i$ to the crystal potential but keeping the energy E real in the Schrödinger equation $\hat{H}\Psi = E\Psi$. (Alternatively, non-hermiticity can be introduced by nonreciprocal hopping in the tight-binding picture [20].) The optical potential $-iV_i$ is associated with the imaginary part of the electron self-energy [21, 22] due to the interaction with the electron environment. This phenomenological description is commonly used in the one-step theory of the stationary photoemission [23, 24] to simulate the surface sensitivity of the measurement and in the theory of LEED to reproduce the shape of the experimental reflection and transmission spectra [25]. Furthermore, the V_i formalism was applied to electron propagation [26] and time-resolved photoemission [22]. In Ref. [22] the results by a time-dependent Schrödinger equation with absorbing potential were compared to the inelastic scattering treated fully microscopically by means of random collisions. In the former approach the dephasing of the wave packet is neglected, while in the latter the observables are obtained from a statistical averaging over random perturbations. The two schemes were found to agree well regarding the delay time in a numerical streaking experiment.

This makes it quite reasonable to try to take advantage of the artificial coherence of the scattering state and apply the EWS formalism also in the presence of the inelas-

tic scattering. Here, we consider transmission and reflection of a wave packet incident on an absorptive potential well within a one-dimensional (1D) jellium model. This problem has an exact analytical solution, which allows to unambiguously establish a rather nontrivial effect of the optical potential on the energy dependence of reflection time delay: at the points of complete transparency on switching on the absorption the $\Delta\tau_{\text{EWS}}(E)$ maxima turn into sharp local minima, which become broader and more shallow with increase of V_i .

The paper is organized as follows: The model is introduced in Sec. II. Section III analyses time delays in the absence of the inelastic scattering. The influence of the absorbing potential is discussed in Sec. IV followed by conclusions in Sec. V. The details of formulae derivation and some explicit expressions are presented in A.

II. MODEL

For a normal incidence on a jellium slab the problem reduces to a textbook 1D problem of a particle scattered by a rectangular potential well. Let the well extend from $z = 0$ to $z = d$, so the Hamiltonian in atomic units $\hbar = e = m = 1$ is

$$\hat{H} = -\frac{1}{2} \frac{\partial^2}{\partial z^2} + V(z), \quad (3)$$

with the potential

$$V(z) = \begin{cases} -U, & 0 \leq z \leq d, \\ 0, & \text{otherwise.} \end{cases} \quad (4)$$

The space is divided into three regions: the half-space to the left of the slab, a finite scattering region, and the half-space to the right of the slab. The solution of the stationary Schrödinger equation $\hat{H}\psi = E\psi$ for a wave incident from the left at a positive energy $E = k^2/2$ is

$$\psi(z) = \begin{cases} e^{ikz} + re^{-ikz}, & z < 0, \\ Ae^{iKz} + Be^{-iKz}, & 0 \leq z \leq d, \\ te^{ikz}, & z > d. \end{cases} \quad (5)$$

In the left half-space the wave function consists of the incident wave of unit amplitude and a reflected wave moving in the opposite direction with the amplitude $r = i|r|\exp(i\eta_r)$. In the scattering region, it is a sum of two waves propagating in opposite directions. For a potential well ($U > 0$), K is larger than the free-space wave vector k . (For a scatterer that is a fragment of a periodic potential these are two Bloch waves with the Bloch vectors K and $-K$.) In the right half-space, there is only the transmitted wave moving to the right with the amplitude $t = |t|\exp(i\eta_t)$.

The amplitudes are found from the condition of the continuity of the function $\psi(z)$ and its derivative $\partial\psi/\partial z$

at the boundaries $z = 0$ and $z = d$, see A:

$$t = \frac{e^{-ikd}}{\cos(Kd) - i\frac{K^2 + k^2}{2kK} \sin(Kd)}, \quad (6)$$

$$r = i\frac{K^2 - k^2}{2kK} \sin(Kd) te^{ikd}, \quad (7)$$

$$A = \frac{K + k}{2K} te^{i(k-K)d} = \frac{K + k + r(K - k)}{2K}, \quad (8)$$

$$B = \frac{K - k}{2K} te^{i(k+K)d} = \frac{K - k + r(K + k)}{2K}. \quad (9)$$

From the stationary wave function of Eq. (5) we now obtain the EWS time delay of the transmitted and reflected wave packets as the energy derivatives of the transmission and reflection phases η_t and η_r derived from Eqs. (6) and (7), respectively.

III. PURELY ELASTIC SCATTERING

First, let us consider a real potential $U = V_0$. Then the wave vectors in the scattering region are also real, $K = \sqrt{2(E + V_0)}$, and Eq. (7) yields the simple relation between the phases of transmission and reflection amplitudes [27]

$$\eta_r = \frac{\pi}{2} + \eta_t + kd. \quad (10)$$

Similar to transmission, Eq. (2), the time delay on reflection $\Delta\tau_r$ equals the energy derivative of the phase shift η_r of the reflected wave, $\Delta\tau_r = \dot{\eta}_r$.

Following Hartman [28] we also introduce the so-called transit time $\tau_t = \Delta\tau_{\text{EWS}} + d/k$, which is the time a classical particle would spend in the scattering region if it obeyed the equations of motion (1). Owing to the relation (10), the reflection time delay coincides with the transit time (recall that $v = k$ in the atomic units):

$$\Delta\tau_r = \Delta\tau_{\text{EWS}} + d/k. \quad (11)$$

The transmission amplitude t in Eq. (6) has the form

$$te^{ikd} = \frac{1}{a - ib}, \quad (12)$$

where real and imaginary parts of the denominator are

$$a = \cos(Kd), \quad b = \frac{K^2 + k^2}{2kK} \sin(Kd). \quad (13)$$

Then the transmission probability $T \equiv |t|^2$ is

$$T = \frac{1}{a^2 + b^2} = \frac{1}{1 + \left[\frac{V_0}{kK} \sin(Kd) \right]^2}. \quad (14)$$

Equation (14) shows that the transmission probability T oscillates as a function of K with the period π/d : There is

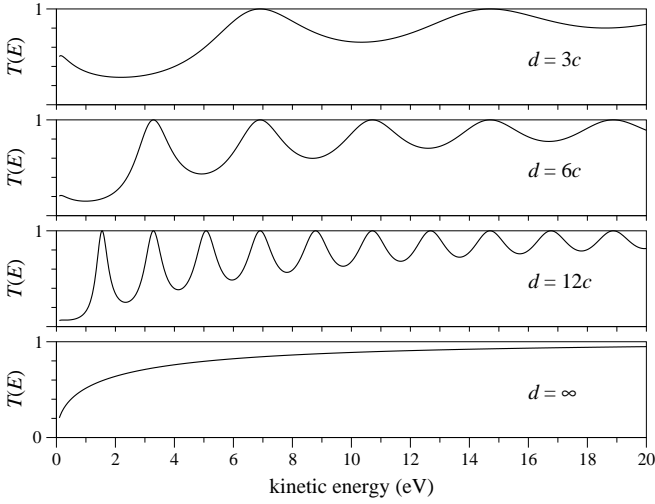


FIG. 1. Energy dependence of the transmission probability $T = |t|^2$ for potential wells of different widths, $d = nc$ with $c = 6.34 a_0$. The potential inside the well is $-U = V_0 = -30.21$ eV. The period of oscillations is π/d .

a finite probability to be reflected from the potential well at all energies except for the transparency resonances. The $T = 1$ resonances occur at $K_n^{\text{res}} = \pi n/d$, where the integer n is greater than $d\sqrt{2V_0}/\pi$, i.e., at the energies $E_n^{\text{res}} = (\pi n/d)^2/2 - V_0$. The phase of the transmission amplitude is then

$$\eta_T + kd = \arctan \frac{d}{a} = \arctan \left[\frac{k^2 + V_0}{kK} \tan(Kd) \right],$$

and the transit time is

$$\begin{aligned} \tau_T &= \eta_T + d/k = |t|^2 (a\dot{b} - b\dot{a}) \\ &= \frac{T}{kK^2} \left[d(k^2 + V_0) - V_0^2 \frac{\sin(2Kd)}{k^2 K} \right]. \end{aligned} \quad (15)$$

Figure 1 shows the energy dependence of the transmission probability $T(E)$ for the scattering regions of different widths d . We have chosen the parameters that roughly model the graphene multilayers studied in Refs. [29–32], namely $c = 6.34 a_0$ and $V_0 = 30.21$ eV. According to Eq. (15), the transit time oscillates between the two envelope functions

$$\tau_T^{\text{max}} = d \frac{(k^2 + V_0)}{kK^2} \quad \text{and} \quad (16)$$

$$\tau_T^{\text{min}} = d \frac{k(k^2 + V_0)}{(kK)^2 + V_0^2} \quad (17)$$

as a result of the multiple reflections from both boundaries of the well [11]. The same behavior for the reflection time delay follows from Eq. (11), see Fig. 2.

Landauer and Martin [15] proposed an approximate formula for the transit time $\tau_{\text{LM}} = d/v_g$, where v_g is the group velocity in the crystal. In our model, $v_g = K$,

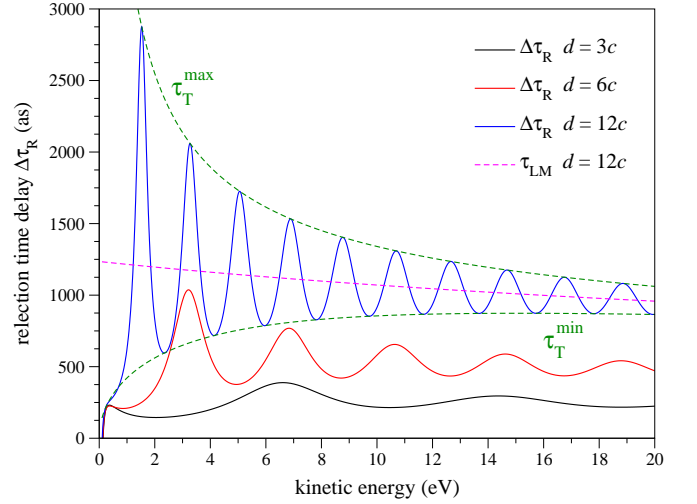


FIG. 2. Reflection time delay $\Delta\tau_r(E) = \tau_r(E)$ for three widths of the potential well, $d = 3c, 6c$, and $12c$ (solid lines). The energy locations of the maxima are close to the those of the $T(E)$ maxima, E_n^{res} . Dashed lines show the envelope functions τ_T^{min} and τ_T^{max} and the Landauer-Martin formula $\tau_{\text{LM}} = d/v_g$, see Eq. (6.2) in Ref. [15].

and τ_{LM} lies between the envelope functions τ_T^{min} and τ_T^{max} . Let us recall that Eq. (15) gives the transit time for the wave packets having the spectral width much smaller than the distance between the maxima of τ_T , i.e., the packets composed of the waves with the energies $|E - E_n^{\text{res}}| \ll (\pi/d)^2(n+1/2)$. One may suppose that the Landauer-Martin formula gives an average time delay for a packet, whose spectral width is larger than the energy distance between the neighboring maxima E_n^{res} . Such a packet may be represented as a sum of spectrally narrow packets, which are transmitted (and reflected) with substantially different delays. Thus, the sum of the transmitted narrow packets have the shape substantially different from the incident packet, and it may even split into several packets. The reflected packet is similarly distorted. Thus, the Landauer-Martin formula cannot be unambiguously interpreted as an average transit time for a spectrally wide packet.

We see from expressions (16) and (17) that the upper and lower limits of τ_T are proportional to the slab width d , and according to Eq. (15) τ_T increases with the width. Now let us consider a slab of infinite width, $d \rightarrow \infty$, i.e., the reflection from a semi-infinite crystal, which in our model means the reflection from a step function. As shown in A, the reflection amplitude

$$r_\infty = \frac{k - K}{k + K} \quad (18)$$

in this case is *real* and, consequently, the reflection time delay *vanishes* instead of the intuitively expected divergence with $d \rightarrow \infty$. So, the reflected wave packet conserves shape and is a reduced copy of the incident packet, with the equation of motion for its maximum being the

same as for the ideally reflected packet, $z_R(t) = -vt$. This is a consequence of the absence of the second boundary: there is no interference with the internally reflected waves.

IV. INCLUSION OF THE ABSORBING POTENTIAL

For a realistic description of scattering, the inelastic processes must be included, to which end we add an imaginary part to the potential in the scatterer: $U = V_0 + iV_i$, see Eqs. (3) and (4). Equations (6)–(9) for the coefficients of the partial waves remain the same, but the wave vector in the slab becomes complex $K = K_1 + iK_2$. It satisfies the equation

$$K^2 = 2(E + V_0 + iV_i), \quad (19)$$

which gives

$$K_1 = \sqrt{\sqrt{(E + V_0)^2 + V_i^2} + E + V_0}, \quad (20)$$

$$K_2 = \frac{V_i}{K_1}. \quad (21)$$

Substituting the complex vector K into Eq. (6) we find the transmission amplitude in the form similar to Eq. (12):

$$te^{ikd} = \frac{1}{p - iq}. \quad (22)$$

The expressions for p and q are more involved than Eq. (13), and they are given in A, Eqs. (A6) and (A7).

Similar to Eq. (15) the transit time is

$$\tau_T = |t|^2(\dot{q}p - q\dot{p}). \quad (23)$$

Explicit expressions for \dot{p} and \dot{q} are given in Eqs. (A8) and (A9) in A.

Figure 3 shows the transit time for different values of V_i for the scatterer width $d = 3c$. The absorbing potential is seen to damp the oscillations of τ_T , which is an expected result of the inclusion of absorbing potential: The $-iV_i$ term leads to a finite imaginary part of the wave vector K inside the slab, whereby the wave function decays into the solid, and the wave incident from the left becomes less sensitive to the presence of the right boundary of the slab. Note a qualitative difference of the effect of the wave function decay due to absorption from the decay due to tunneling: In the latter case the transit time becomes independent on the width d leading to nominally unlimited propagation velocities—the famous Hartman effect [28].

Let us now consider reflection. For a perfectly reflecting impenetrable plane at $z = 0$ the equation of motion for the maximum of the reflected wave packet is $z_R(t) = -vt$, and the scatterer is characterized by the reflection time delay $\Delta\tau_R$ that modifies the equation of motion: $z_R(t) = -v(t - \Delta\tau_R)$. The effect of V_i on the timing

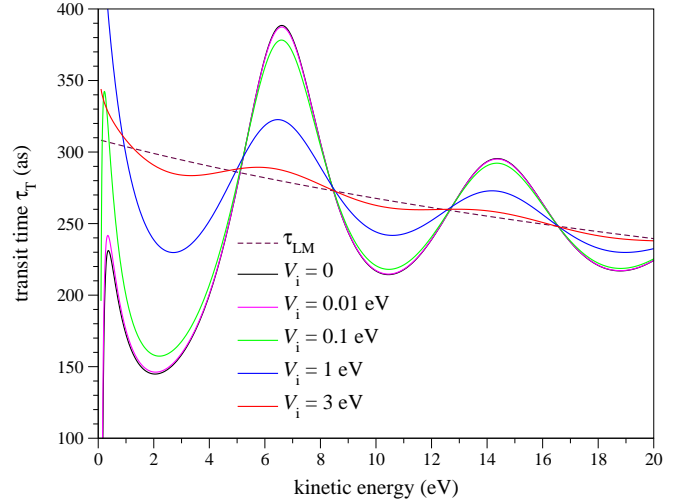


FIG. 3. Transit time τ_T for a slab width $d = 3c$ for five values of the absorbing potential $V_i = 0, 0.01, 0.1, 1$, and 3 eV (solid lines). The real part of the potential is $V_0 = 30.21$ eV, as in Figs. 1 and 2. Dashed curve is the Landauer-Martin time $\tau_{LM} = d/v_g$.

of the reflected wave packet is rather unexpected. In contrast to the elastic case, for a finite V_i the reflection time delay $\Delta\tau_R$ does not equal the transit time. Equation (11) does not hold because the relation (10) between the reflection and transmission phases is valid only for real K . The reason is the energy dependence of the imaginary part of K , see Eq. (21), which results in the energy dependence of the phases of all the terms in Eq. (7). Thus, for a finite V_i , instead of Eq. (10) we have

$$\eta_R = \frac{\pi}{2} + \eta_1 + \eta_2 + \eta_T + kd, \quad (24)$$

where

$$\eta_1 = \arg \frac{K^2 - k^2}{2kK} = \arctan \frac{b_1}{a_1}, \quad (25)$$

$$a_1 = K_1(|K|^2 - k^2),$$

$$b_1 = K_2(|K|^2 + k^2)$$

$$\eta_2 = \arg [\sin(Kd)] = \arctan \frac{b_2}{a_2} \quad (26)$$

$$a_2 = \tan(K_1 d)$$

$$b_2 = \tanh(K_2 d).$$

Then, the reflection delay $\Delta\tau_R$ is the sum of the transit time τ_T and two additional terms

$$\Delta\tau_R = \dot{\eta}_1 + \dot{\eta}_2 + \tau_T, \quad (27)$$

where

$$\begin{aligned}\dot{\eta}_i &= \frac{a_i \dot{b}_i - b_i \dot{a}_i}{a_i^2 + b_i^2}, \\ \dot{a}_1 &= (3K_1^2 + K_2^2 - k^2)\dot{K}_1 + 2K_1(K_2\dot{K}_2 - 1), \\ \dot{b}_1 &= (3K_2^2 + K_1^2 + k^2)\dot{K}_2 + 2K_2(K_1\dot{K}_1 + 1), \\ \dot{a}_2 &= \frac{d\dot{K}_1}{\cos^2(K_1 d)}, \\ \dot{b}_2 &= \frac{d\dot{K}_2}{\cosh^2(K_2 d)}.\end{aligned}$$

The delay $\dot{\eta}_1$ does not depend on the width d and becomes small compared to the transit time with the increase of the width. The delay $\dot{\eta}_2$ is comparable to the transit time because it is proportional to d . It is instructive to expand the delay near a point of complete transparency $K_n^{\text{res}} = \pi n/d$ for $V_i = 0$. We set $K_1 = K_n^{\text{res}} + \Delta K$ with $\Delta K d \ll 1$ and assume, quite realistically, that $V_i/V_0 \ll 1$. Then

$$\begin{aligned}\dot{\eta}_2 &= \frac{d}{\tan^2(K_1 d) + \tanh^2(K_2 d)} \left[\frac{\tan(K_1 d)\dot{K}_2}{\cosh^2(K_2 d)} \right. \\ &\quad \left. - \frac{\tanh(K_2 d)\dot{K}_1}{\cos^2(K_1 d)} \right] \approx -\frac{V_i}{(K_n^{\text{res}} \Delta K)^2 + V_i^2}.\end{aligned}\quad (28)$$

We see that near the maxima of $\tau_T(E)$, with $\Delta K \rightarrow 0$, the reflection delay strongly deviates from its $V_i = 0$ shape owing to the large negative term $\dot{\eta}_2(K_n^{\text{res}}) \sim -1/V_i$. This is illustrated in Fig. 4, where the reflection time delay is shown for the same set of parameters as in Fig. 3. As follows from Eq. (28), in the vicinity of the resonance, the reflection time delay $\tau_R(E)$ strongly deviates from $\tau_T(E)$ showing a deep minimum, which is the sharper the smaller V_i . This instability is apparently an artifact of the optical-potential-based phenomenology, and it points to its limitations: Indeed, the divergent time delay at $V_i \rightarrow 0$ can hardly be ascribed a physical meaning.

Furthermore, in the limit of semi-infinite crystal, the energy dependent imaginary part of K caused by the absorbing potential leads to a finite reflection time delay because the reflection amplitude r_∞ in Eq. (18) becomes complex. Figure 5 shows the reflection time delay for a fixed value of $V_i = 3$ eV for different slab widths. As one would expect, in the presence of the absorbing potential, with the increase of the slab width d the reflection time delay steadily converges to its value for the semi-infinite well.

V. CONCLUSION

The present study demonstrates that the theory of attosecond dynamics requires a careful analysis of the phenomenology that underlies the calculations. In particular, we have studied the effect of the absorbing potential

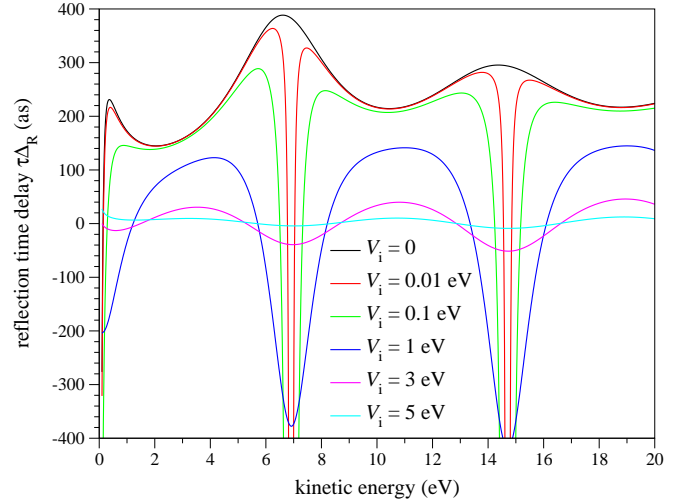


FIG. 4. Reflection time delay τ_R for $d = 3c$ and six values of absorbing potential $V_i = 0, 0.01, 0.1, 1, 3$, and 5 eV.

on the phase time (EWS delay) of the transmitted and reflected wave packet. For the transmitted packet the effect of V_i is to damp out the oscillations of the transit time. Thereby in the limit $V_i \rightarrow \infty$ the oscillating $\tau_T(E)$ curve converges to the intuitively understandable Landauer-Martin curve.

Contrastingly, for the reflected packet the effect is rather counterintuitive: as a function of V_i , the time delay $\tau_R(E)$ shows a discontinuity at its maxima, with $\tau_R(E^{\text{max}}) \rightarrow -\infty$ at $V_i \rightarrow 0$. Furthermore, at realistic values of V_i the reflection delay shows appreciably large negative values (i.e., time advance) over an energy interval of tenths of eV. This behavior is common to transmission resonances in various 1D systems, and here we have demonstrated it for a simple system amenable to analyt-

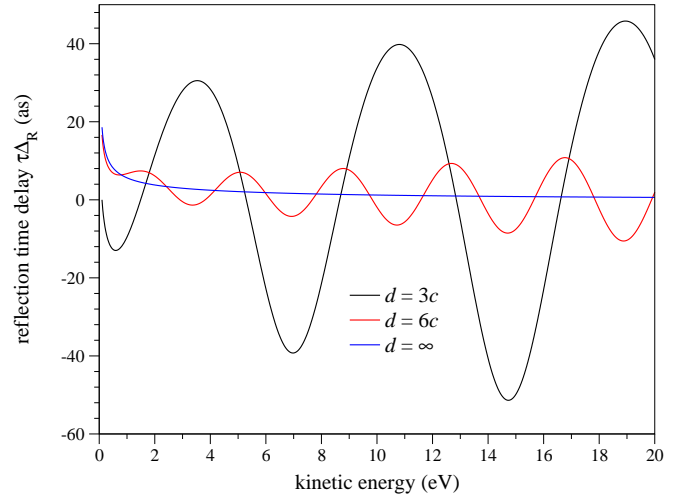


FIG. 5. Reflection time delay τ_R for the absorbing potential value $V_i = 3$ eV, and the well width $d = 3c$ and $6c$, as well as for the semi-infinite well $d = \infty$.

ical treatment and obtained the exact expressions (27) and (28), leaving no doubts as to the validity of this result.

The large negative delays do not seem to have physical meaning, which raises some concerns regarding the applicability of the EWS formalism in combination with the phenomenology of optical potential. In view of the wide application of both concepts in transport, LEED, and photoemission theories, this calls for seeking out alternative ways of allowing for the inelastic scattering. This is quite challenging because, for example, introducing the non-hermiticity by means of nonreciprocal hopping is limited to the tight-binding representation, which is not applicable above the vacuum level. Generally, it is not clear how to reconcile the actual dephasing of the wave packet with the phase-time formalism. In any case, in using the absorbing-potential approach it is important to be aware of possible potholes and carefully check the physical consistency of the results. To our knowledge, the V_i -related spurious features of LEED are here revealed for the first time, and we hope the present study to draw further attention to the problem.

ACKNOWLEDGMENTS

This work was supported by the Spanish Ministry of Science and Innovation (MICINN Project No. PID2022-139230NB-I00) and by the National Academy of Sciences of Ukraine (Project No. III-2-22 and III-4-23).

Appendix A: Details of derivation

The condition of the continuity of the function $\psi(z)$ and its derivative $\partial\psi/\partial z$ at $z = 0$ is

$$\begin{cases} 1 + r &= A + B, \\ k(1 - r) &= K(A - B). \end{cases} \quad (\text{A1})$$

The continuity at $z = d$ yields

$$\begin{cases} Ae^{ikd} + Be^{-iKd} &= te^{ikd} \\ K(Ae^{iKd} - Be^{-iKd}) &= kte^{ikd}. \end{cases} \quad (\text{A2})$$

$$\begin{aligned} \sin(Kd) &= \sin(K_1d) \cosh(K_2d) + i \cos(K_1d) \sinh(K_2d), \\ \cos(Kd) &= \cos(K_1d) \cosh(K_2d) - i \sin(K_1d) \sinh(K_2d), \end{aligned}$$

etc. The transmission amplitude now has the form (22), similar to (12), but the expressions for p and q become formidable

$$p = \cos(K_1d) \left[\cosh(K_2d) + \frac{K_1}{2} \left(\frac{1}{k} + \frac{k}{|K|^2} \right) \sinh(K_2d) \right] + \frac{K_2}{2} \left(\frac{1}{k} - \frac{k}{|K|^2} \right) \sin(K_1d) \cosh(K_2d), \quad (\text{A6})$$

$$q = \sin(K_1d) \left[\sinh(K_2d) + \frac{K_1}{2} \left(\frac{1}{k} + \frac{k}{|K|^2} \right) \cosh(K_2d) \right] - \frac{K_2}{2} \left(\frac{1}{k} - \frac{k}{|K|^2} \right) \cos(K_1d) \sinh(K_2d). \quad (\text{A7})$$

Excluding $t \exp(ikd)$ from the system (A2), we obtain

$$K(Ae^{iKd} - Be^{-iKd}) = k(Ae^{iKd} + Be^{-iKd}),$$

which gives the relation between the amplitudes A and B :

$$B = Ae^{iKd} \frac{K - k}{K + k}.$$

Then from the first equation of the system (A2) we express A via $t \exp(ikd)$. Finally we find the expressions (8) and (9) for both amplitudes:

$$A = \frac{K + k}{2K} te^{i(k-K)d}, \quad (\text{A3})$$

$$B = \frac{K - k}{2K} te^{i(k+K)d}. \quad (\text{A4})$$

We rewrite the system (A1) as

$$\begin{cases} 1 + r &= A + B, \\ 1 - r &= \frac{K}{k}(A - B). \end{cases} \quad (\text{A5})$$

By substituting Eqs. (A3) and (A4) into the system (A5) we obtain Eq. (6) from the sum of the two equations (A5) and Eq. (7) from their difference. Further, we obtain the equations (8)–(9).

The reflection from the half space is considered similarly. The region $z > d$ is absent, and the solution in the right half-space is $\psi(z) = A \exp(iKz)$. The only boundary condition is at $z = 0$; it is given by Eqs. (A1) with $B = 0$. This immediately yields $k(1 - r_\infty) = K(1 + r_\infty)$, which leads to Eq. (18).

The boundary conditions (A1) and (A2) are the same for real and complex U . Thus, the expressions for the wave function coefficients (6)–(9) have the same form in the presence of absorbing potential $-iV_i$. However, the wave vector inside the slab becomes complex, $K = K_1 + iK_2$, and the dependence of the phases of the coefficients on energy becomes more sophisticated:

For the calculation of the transit time, Eq. (23), we need the energy derivatives of these terms

$$\begin{aligned} \dot{p} = & -\sin(K_1 d) d\dot{K}_1 \left[\cosh(K_2 d) + \frac{K_1}{2} \left(\frac{1}{k} + \frac{k}{|K|^2} \right) \sinh(K_2 d) \right] \\ & + \cos(K_1 d) \left\{ \sinh(K_2 d) d\dot{K}_2 + \frac{\partial}{\partial E} \left[\frac{K_1}{2} \left(\frac{1}{k} + \frac{k}{|K|^2} \right) \right] \sinh(K_2 d) + \frac{K_1}{2} \left(\frac{1}{k} + \frac{k}{|K|^2} \right) \cosh(K_2 d) d\dot{K}_2 \right\} \\ & + \frac{\partial}{\partial E} \left[\frac{K_2}{2} \left(\frac{1}{k} - \frac{k}{|K|^2} \right) \right] \sin(K_1 d) \cosh(K_2 d) \\ & + \frac{K_2}{2} \left(\frac{1}{k} - \frac{k}{|K|^2} \right) [\cos(K_1 d) d\dot{K}_1 \cosh(K_2 d) + \sin(K_1 d) \sinh(K_2 d) d\dot{K}_2], \end{aligned} \quad (\text{A8})$$

where

$$\begin{aligned} \frac{\partial}{\partial E} \left[\frac{K_1}{2} \left(\frac{1}{k} + \frac{k}{|K|^2} \right) \right] &= \frac{\dot{K}_1}{2} \left(\frac{1}{k} + \frac{k}{|K|^2} \right) + \frac{K_1}{2} \left[-\frac{1}{k^3} + \frac{1}{k|K|^2} - \frac{2k}{|K|^4} (K_1 \dot{K}_1 + K_2 \dot{K}_2) \right], \\ \frac{\partial}{\partial E} \left[\frac{K_2}{2} \left(\frac{1}{k} - \frac{k}{|K|^2} \right) \right] &= \frac{\dot{K}_2}{2} \left(\frac{1}{k} - \frac{k}{|K|^2} \right) + \frac{K_2}{2} \left[-\frac{1}{k^3} - \frac{1}{k|K|^2} + \frac{2k}{|K|^4} (K_1 \dot{K}_1 + K_2 \dot{K}_2) \right], \end{aligned}$$

and

$$\begin{aligned} \dot{q} = & \cos(K_1 d) d\dot{K}_1 \left[\sinh(K_2 d) + \frac{K_1}{2} \left(\frac{1}{k} + \frac{k}{|K|^2} \right) \cosh(K_2 d) \right] \\ & + \sin(K_1 d) \left\{ \cosh(K_2 d) d\dot{K}_2 + \frac{\partial}{\partial E} \left[\frac{K_1}{2} \left(\frac{1}{k} + \frac{k}{|K|^2} \right) \right] \cosh(K_2 d) + \frac{K_1}{2} \left(\frac{1}{k} + \frac{k}{|K|^2} \right) \sinh(K_2 d) d\dot{K}_2 \right\} \\ & - \frac{\partial}{\partial E} \left[\frac{K_2}{2} \left(\frac{1}{k} - \frac{k}{|K|^2} \right) \right] \cos(K_1 d) \sinh(K_2 d) \\ & - \frac{K_2}{2} \left(\frac{1}{k} - \frac{k}{|K|^2} \right) [-\sin(K_1 d) d\dot{K}_1 \sinh(K_2 d) + \cos(K_1 d) \cosh(K_2 d) d\dot{K}_2]. \end{aligned} \quad (\text{A9})$$

-
- [1] A. L. Cavalieri, N. Mueller, T. Uphues, V. S. Yakovlev, A. Baltuska, B. Horvath, B. Schmidt, L. Bluemel, R. Holzwarth, S. Hendel, M. Drescher, U. Kleineberg, P. M. Echenique, R. Kienberger, F. Krausz, and U. Heinzmann, Attosecond spectroscopy in condensed matter, *Nature* **449**, 1029 (2007).
- [2] M. Schultze, M. Fieß, N. Karpowicz, J. Gagnon, M. Korbman, M. Hofstetter, S. Neppl, A. L. Cavalieri, Y. Komninos, T. Mercouris, C. A. Nicolaides, R. Pazourek, S. Nagele, J. Feist, J. Burgdörfer, A. M. Azzeer, R. Ernstorfer, R. Kienberger, U. Kleineberg, E. Goulielmakis, F. Krausz, and V. S. Yakovlev, Delay in photoemission, *Science* **328**, 1658 (2010).
- [3] S. Neppl, R. Ernstorfer, E. M. Bothschafter, A. L. Cavalieri, D. Menzel, J. V. Barth, F. Krausz, R. Kienberger, and P. Feulner, Attosecond time-resolved photoemission from core and valence states of magnesium, *Phys. Rev. Lett.* **109**, 087401 (2012).
- [4] S. Neppl, R. Ernstorfer, A. L. Cavalieri, C. Lemell, G. Wachter, E. Magerl, E. M. Bothschafter, M. Jobst, M. Hofstetter, U. Kleineberg, J. V. Barth, D. Menzel, J. Burgdörfer, P. Feulner, F. Krausz, and R. Kienberger, Direct observation of electron propagation and dielectric screening on the atomic length scale, *Nature* **517**, 342 (2015).
- [5] W. A. Okell, T. Witting, D. Fabris, C. A. Arrell, J. Hengster, S. Ibrahimkuty, A. Seiler, M. Barthelmess, S. Stankov, D. Y. Lei, Y. Sonnefraud, M. Rahmani, T. Uphues, S. A. Maier, J. P. Marangos, and J. W. G. Tisch, Temporal broadening of attosecond photoelectron wavepackets from solid surfaces, *Optica* **2**, 383 (2015).
- [6] F. Siek, S. Neb, P. Bartz, M. Hensen, C. Strüber, S. Fiechter, M. Torrent-Sucarrat, V. M. Silkin, E. E. Krasovskii, N. Kabachnik, S. Fritzsche, R. D. M. no, P. M. Echenique, A. K. Kazansky, N. Müller, W. Pfeiffer, and U. Heinzmann, Angular momentum-induced delays in solid-state photoemission enhanced by intra-atomic interactions, *Science* **357**, 1274 (2017).
- [7] M. Ossiander, J. Riemensberger, S. Neppl, M. Mittermair, M. Schäffer, A. Duensing, M. S. Wagner, R. Heider, M. Wurzer, M. Gerl, M. Schnitzenbaumer, J. V. Barth, F. Libisch, C. Lemell, J. Burgdörfer, P. Feulner, and R. Kienberger, Absolute timing of the photoelectric effect, *Nature* **561**, 374 (2018).
- [8] J. Riemensberger, S. Neppl, D. Potamianos, M. Schäffer, M. Schnitzenbaumer, M. Ossiander, C. Schröder, A. Guggenmos, U. Kleineberg, D. Menzel, F. Allegretti, J. V. Barth, R. Kienberger, P. Feulner, A. G. Borisov,

- P. M. Echenique, and A. K. Kazansky, Attosecond dynamics of *sp*-band photoexcitation, *Phys. Rev. Lett.* **123**, 176801 (2019).
- [9] R. Locher, L. Castiglioni, M. Lucchini, M. Greif, L. Gallmann, J. Osterwalder, M. Hengsberger, and U. Keller, Energy-dependent photoemission delays from noble metal surfaces by attosecond interferometry, *Optica* **2**, 405 (2015).
- [10] Z. Tao, C. Chen, T. Szilvási, M. Keller, M. Mavrikakis, H. Kapteyn, and M. Murnane, Direct time-domain observation of attosecond final-state lifetimes in photoemission from solids, *Science* **353**, 62 (2016).
- [11] D. Bohm, *Quantum Theory* (Prentice-Hall, New York, 1951).
- [12] E. P. Wigner, Lower limit for the energy derivative of the scattering phase shift, *Phys. Rev.* **98**, 145 (1955).
- [13] F. T. Smith, Lifetime matrix in collision theory, *Phys. Rev.* **118**, 349 (1960).
- [14] E. H. Hauge and J. A. Støvneng, Tunneling times: a critical review, *Rev. Mod. Phys.* **61**, 917 (1989).
- [15] R. Landauer and T. Martin, Barrier interaction time in tunneling, *Rev. Mod. Phys.* **66**, 217 (1994).
- [16] H. G. Winful, Tunneling time, the Hartman effect, and superluminality: A proposed resolution of an old paradox, *Physics Reports* **436**, 1 (2006).
- [17] G. E. Field, On the status of quantum tunnelling time, *European Journal for Philosophy of Science* **12**, 57 (2022).
- [18] P. J. Feibelman and D. E. Eastman, Photoemission spectroscopy—correspondence between quantum theory and experimental phenomenology, *Phys. Rev. B* **10**, 4932 (1974).
- [19] J. C. Slater, Damped electron waves in crystals, *Phys. Rev.* **51**, 840 (1937).
- [20] S. Longhi, Non-Hermitian Hartman Effect, *Annalen der Physik* **534**, 2200250 (2022).
- [21] D. W. Jepsen, F. J. Himpsel, and D. E. Eastman, Single-step-model analysis of angle-resolved photoemission from Ni(110) and Cu(100), *Phys. Rev. B* **26**, 4039 (1982).
- [22] E. E. Krasovskii, C. Friedrich, W. Schattke, and P. M. Echenique, Rapid propagation of a Bloch wave packet excited by a femtosecond ultraviolet pulse, *Phys. Rev. B* **94**, 195434 (2016).
- [23] J. Pendry, Theory of photoemission, *Surface Science* **57**, 679 (1976).
- [24] J. Braun, The theory of angle-resolved ultraviolet photoemission and its applications to ordered materials, *Reports on Progress in Physics* **59**, 1267 (1996).
- [25] E. E. Krasovskii, W. Schattke, V. N. Strocov, and R. Claessen, Unoccupied band structure of NbSe₂ by very low-energy electron diffraction: Experiment and theory, *Phys. Rev. B* **66**, 235403 (2002).
- [26] F. Delgado, J. G. Muga, and A. Ruschhaupt, Ultrafast propagation of schrödinger waves in absorbing media, *Phys. Rev. A* **69**, 022106 (2004).
- [27] J. P. Falck and E. H. Hauge, Larmor clock reexamined, *Phys. Rev. B* **38**, 3287 (1988).
- [28] T. E. Hartman, Tunneling of a wave packet, *J. Appl. Phys.* **33**, 3427 (1962).
- [29] J. Jobst, A. J. Van Der Torren, E. E. Krasovskii, J. Balgley, C. R. Dean, R. M. Tromp, and S. J. Van Der Molen, Quantifying electronic band interactions in van der waals materials using angle-resolved reflected-electron spectroscopy, *Nat. Commun.* **7**, 13621 (2016).
- [30] E. Krasovskii, Ab initio theory of photoemission from graphene, *Nanomaterials* **11**, 1212 (2021).
- [31] E. Krasovskii, One-step theory view on photoelectron diffraction: Application to graphene, *Nanomaterials* **12**, 4040 (2022).
- [32] E. E. Krasovskii and R. O. Kuzian, Negative transit time in non-tunneling electron transmission through graphene multilayers (2024), to be published.